Spontaneous Redistribution upon Oxidation of a *Bis*-Stibinoarylamine

Alex J. Kosanovich[†]*, Jovanny J. Contreras*[†]*, Nattamai Bhuvanesh, and Oleg V. Ozerov**

Department of Chemistry, Texas A&M University, 3255 TAMU, College Station, TX 77842, USA.

[†] *These authors contributed equally*

ozerov@chem.tamu.edu

ABSTRACT. Oxidation of a bis-stibinoaryl amine (**2**) with chloranil leads first to formation of a crystallographically observed bis-stiboranoraryl amine (**3a**) which then undergoes isomerization to an ionic tetraarylstibonium antimonate (**3b**). The isomerization proceeds at different rates in different solvent, but a univariate explanation of solvent effects is not evident. The antimonate anion in **3b** can be exchanged for a fluoride resulting in a neutral fluorostiborane (**4**), and further to a triflate in an ionic tetraarylstibonium triflate (**5**). Compound **5** displays strong binding of fluoride in tetrahydrofuran. Structures of **3a**, **3b**, **4**, and **5** were determined by single-crystal X-ray diffraction.

Graphical abstract and Synopsis:

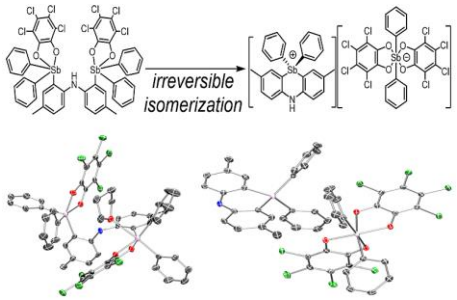

Oxidation of bis(*ortho*-stibinoaryl)amine with chloranil leads to a bis(stiborane) molecule that spontaneously undergoes irreversible transformation into an ionized, cyclized stibonium antimonate isomer.

Keywords: antimony, isomerization, oxidation, fluoride, stibonium

1. Introduction

Compounds of antimony (Sb) have recently received increased attention and development as multifaceted ligands for transition metals with direct metal-Sb bonding [1-5],as remote, redox-active modifiers of classical ligand types [6], and anion sensing [7-12].In particular, we were intrigued by the two examples developed by the by the Gabbaï group for fluoride capture studies (**A** and **B**, Figure 1) [13,14]. These molecules contain two stiborane units that cooperate in capturing the fluoride anion. The stiboranes were obtained via oxidation of the trivalent antimony precursors with *o*-chloranil (3,4,5,6-tetracholoro-*o*-quinone). Compound **B** was found to be superior to **A**, ostensibly because the central oxygen in **A** can provide only a repulsive interaction with fluoride, whereas the central C-H in **B** can provide an attractive C-H…F hydrogen bonding interaction. Because of our past studies with diarylamine-centered pincer ligands [15], we surmised that a bis(stiborane) molecule analogous to **A** and **B**, but with a central NH unit might possess even more affinity for capturing fluoride. The Gabbai group reported a relevant compound **C** in 2023, but did not explore its oxidation with *o*-chloranil [16]. We recently reported transition metal complexes (e.g., **E**) of a PNSb ligand **D** [17]. In this work, we endeavored to synthesize an "SbNSb" analog in order to oxidize to a bis(stiborane) by the Gabbai *o*-chloranil method and assess its fluoride affinity. Although this synthetic approach was successful, the targeted bis(stiborane) underwent an irreversible isomerization that prevented us from studying its fluoride affinity and which we present in this report.

Figure 1. Gabbai's fluoride capture agents and diarylamido-centered pincers.

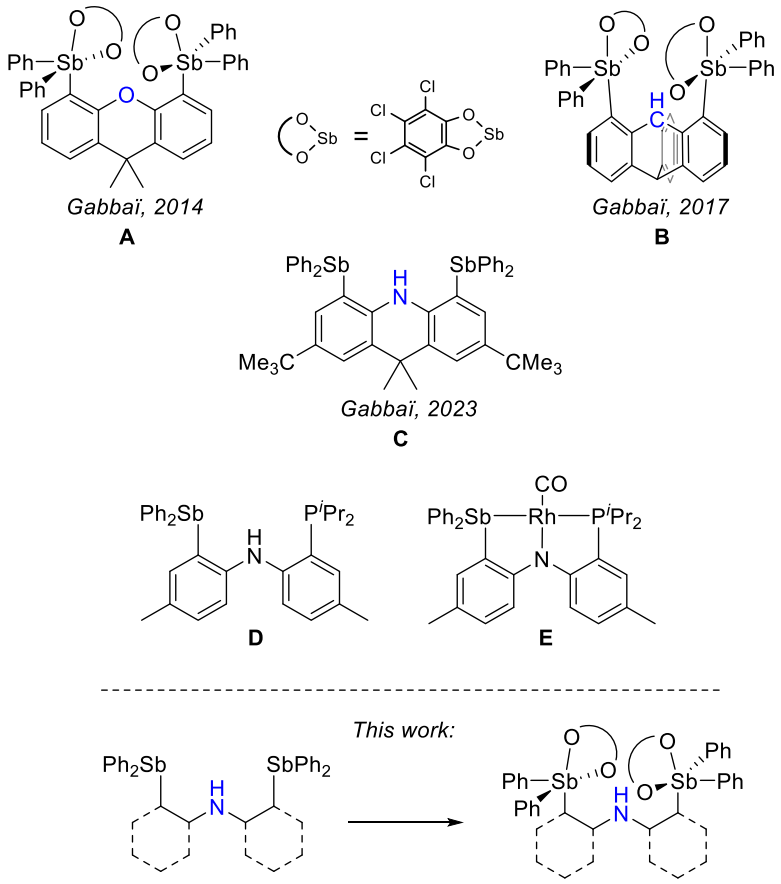

2. Results and Discussion

2.1. Syntheses of bis(antimony) compounds

Treatment of **1** with three equivalents of butyllithium, followed by addition of two equivalents Ph_2SbCl and an aqueous workup, led to the isolation of **2** in 31% yield as a free-flowing, white solid (Scheme 1). ^1H and $^{13}C\{^1H\}$ NMR analysis was consistent with the expected C_{2v} symmetry. The presence of the N-H moiety was confirmed by the observation of an ^1H NMR resonance at δ 5.68 ppm in C_6D_6 and of the N-H stretch by IR spectroscopy at 3338 cm^{-1}.

Scheme 1. Synthesis of compounds **2**-**5**.

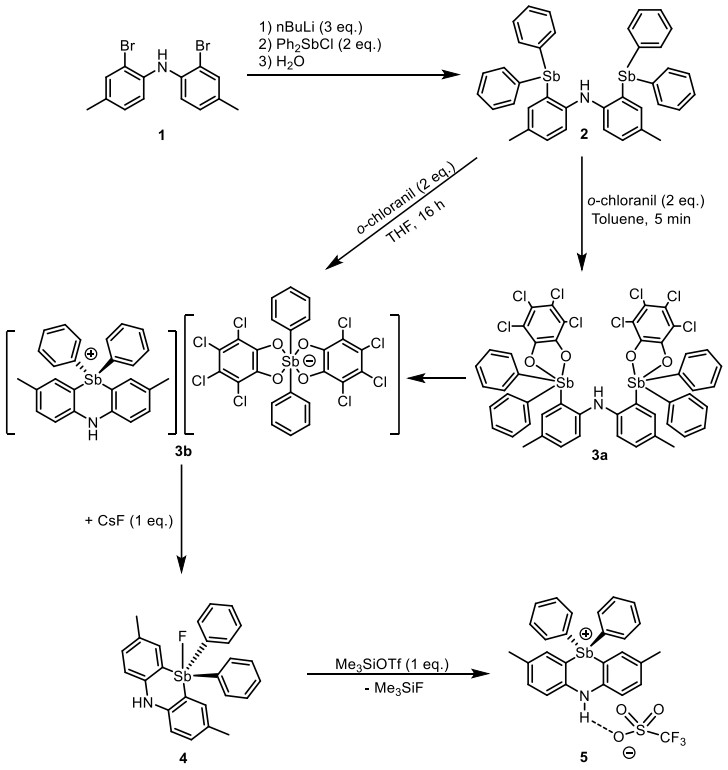

Treatment of **2** with *o*-chloranil in toluene caused an initial color change of the colorless solution to orange, then finally to yellow within 5 minutes. After removal of volatiles and washing with pentane, **3a** was isolated as a pale-yellow solid in 83% yield. Characterization by ^1H NMR spectroscopy in C_6D_6 revealed a downfield shift of the N–H resonance from δ 5.68 ppm to 9.03 ppm, along all other resonances under the expected C_{2v} symmetry. It was noted that longer reaction times (in toluene solvent) led to the formation of precipitate which we later determined to be an

isomerization product. In addition, the use of chloranil that had been stored at ambient temperature for an extended period of time appeared to lead to a faster, unavoidable formation of this new product. We were able to prepare it reproducibly via treatment of **2** with *o*-chloranil in THF for 16 h, resulting in a 92% yield after workup. This new compound was identified as **3b**, a cyclized and ionized isomer of **3a**. ^{1}H NMR analysis in DMSO-d_6 revealed the presence of a downfield N–H resonance at δ 9.79, several much sharper Ph resonances, and a single resonance for the Ar-CH_3 hydrogens.

Scheme 2. Previous examples of ionizing rearrangements of catecholate-containing stiboranes to stibonium antimonate salts.

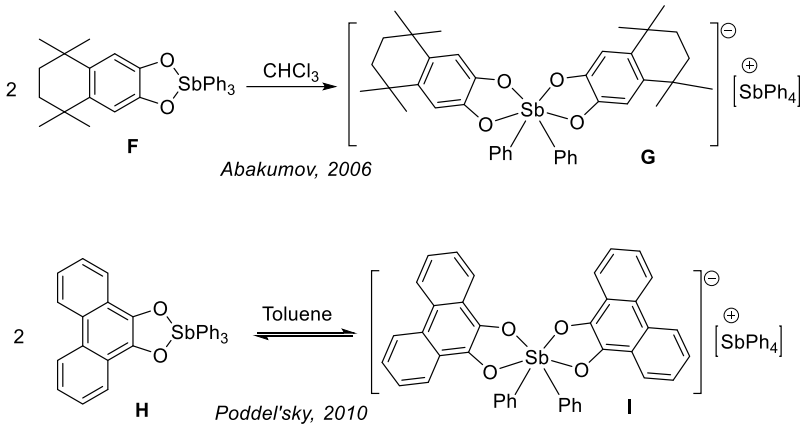

2.2. Isomerization studies of **3a**

Compounds **3a** and **3b** can be observed as distinct, simultaneously present species by ^{1}H NMR spectroscopy in a variety of solvents (vide infra) at ambient temperature. In addition, a variable temperature NMR study of 3b detected no changes at 0, -20, or -40 °C compared to ambient temperature. These observations rule out the possibility that **3a** and **3b** are in rapid equilibrium on the NMR timescale, and thus the isomerization of **3a** into **3b** is irreversible. The observed redistribution of Sb substituents represents a non-redox disproportionation of a five-coordinate, pentavalent Sb with one bidentate catecholate and three aryl substituents into a tetraarylstibonium

with a four-coordinate Sb, and an antimonate with a six-coordinate Sb. Analogous ligand redistribution reactions of related Sb(V) tris(aryl)/catecholates have been previously observed to occur (Scheme 2) [18,19]. In those examples, the isomerization was favorable in the more polar solvents (chloroform or acetone), but reversible in the less polar toluene. In our case, the isomerization is likely more favorable because of entropic reasons (a single molecule of **3a** contains both five-coordinate Sb centers as opposed to two molecules of **F** or **H** engaged in the isomerization).

To understand whether the isomerization rate was affected by the solvent nature, **3a** was dissolved in a series of solvents and its isomerization into **3b** was tracked via ^{1}H NMR spectroscopy. The isomerization reactions appeared to follow a first-order decay (Figure 2) and the relative rates were in the following order: THF-d_8 > CD_2Cl_2 > $CDCl_3$ ≈ C_6D_6 > DMSO-d_6. The isomerization was essentially complete in THF in <1 d and in CD_2Cl_2 in ca. 3 d, but was not complete in the other solvents even after a week. These findings do not allow to make a generalized interpretation based on either the solvent polarity or the coordinating ability of the solvent: DMSO and THF would be the two most polar and most coordinating, but they are at the opposite ends of the rate range. In addition, we cannot exclude that the transformation is catalyzed by adventitious impurities, such as water, or traces of an additional Sb Lewis acidic species present.

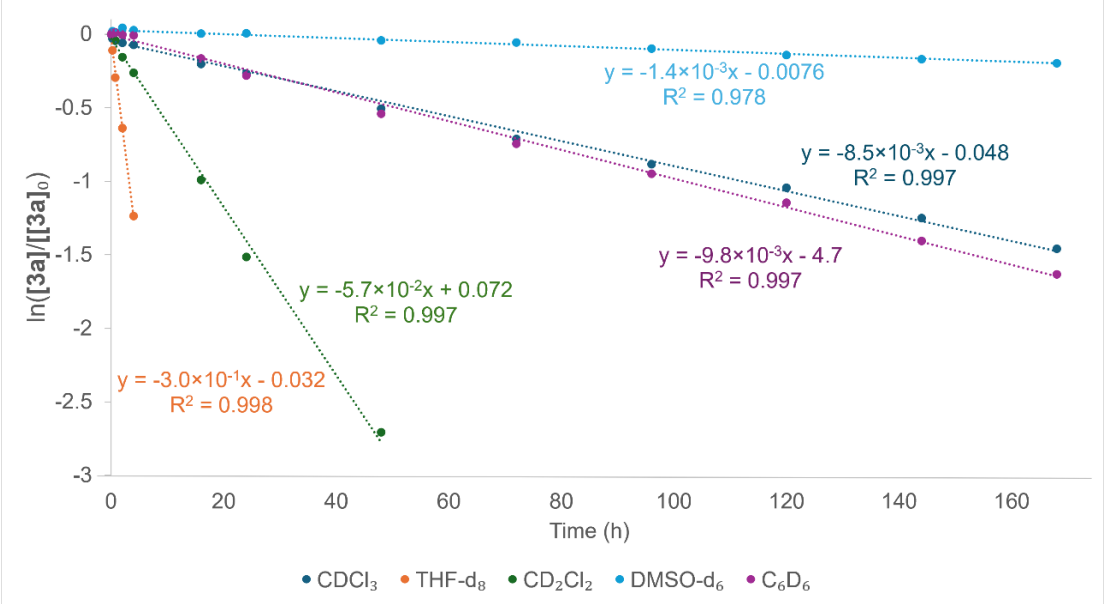

Figure 2. Plot of ln[**3a**]/[**3a**]$_0$ vs time (h) for the isomerization of **3a** to **3b** in different solvents at room temperature.

*2.3. Fluoride Capture Studies of **3b***

Because of the easily occurring rearrangement to **3b**, we did not pursue the studies of fluoride capture with **3a**. However, we wish to investigate the fluoride affinity of the cation in **3b**. In order to exchange the anion in **3b**, it was first treated with one equivalent of CsF in THF causing an immediate change to a clear, homogeneous solution. After the removal of volatiles, and extraction with PhF, **4** was isolated in 84% yield as a free-flowing white powder (Scheme 1). Given the high isolated yield of **4**, we assume by stoichiometry that the by-product of its formation is the Cs salt of the antimonate anion in **3b**, but we made no effort to characterize it. The ^{19}F NMR spectrum in $CDCl_3$ featured a single resonance at δ -100.4 ppm, confirming the presence of the Sb-F bond. The N-H proton resonated at 6.68 ppm in $CDCl_3$ and at 8.31 ppm in THF-d_8. The solid-state structure of 4 (*vide infra*) is dissymmetric, but the ^{1}H and ^{13}C{^{1}H} NMR spectra of **4** in THF-d_8 were consistent with a time-averaged C_{2v} symmetry. One of the ^{1}H NMR aromatic resonances, however, was distinctly broad. In $CDCl_3$, this ^{1}H resonance was missing, presumably broadened beyond

detection, and the $^{13}C\{^{1}H\}$ spectrum contained broader resonances, as well. These observations indicate that the symmetrizing fluxionality in **4** is faster in THF than in chloroform.

Reaction of **4** with Me_3SiOTf led to the release of an equivalent of free Me_3SiF and formation of **5**, which was characterized by multinuclear spectroscopy as well as X-ray diffractometry. ^{1}H NMR observations support the identity of the cation with a downfield N-H resonance at δ 9.55 ppm (in $CDCl_3$), along with all expected aromatic and benzylic (δ 2.22 ppm, 6H) resonances. **5** exhibits a singlet in the ^{19}F NMR spectrum at δ -76.9 ppm corresponding to the triflate anion. Structural analysis revealed a hydrogen bonding interaction between the N-H and an oxygen atom of the triflate anion (N--O distance of ca. 2.91 Å) (Figure 4).

Fluoride anion titrations with monitoring *via* UV-Vis spectroscopy have been successfully utilized by the Gabbai group in order to determine the equilibrium fluoride binding constant, K_f, of various antimony-based Lewis acids [20,21]. Spectrophotometric data collected from the titration of a 3.2 x 10^{-5} M THF solution of **5** with a 0.01 M THF solution of $[^{n}Bu_4N][F]$ (Figure 3) could be accurately fitted to a 1:1 binding isotherm showing formation of the fluoride adduct, **4** (See supporting information). Compound **5** was determined to have a large fluoride binding constant of $K_f > 10^7$, which is consistent with other tetraarylstibonium species in organic media [22].

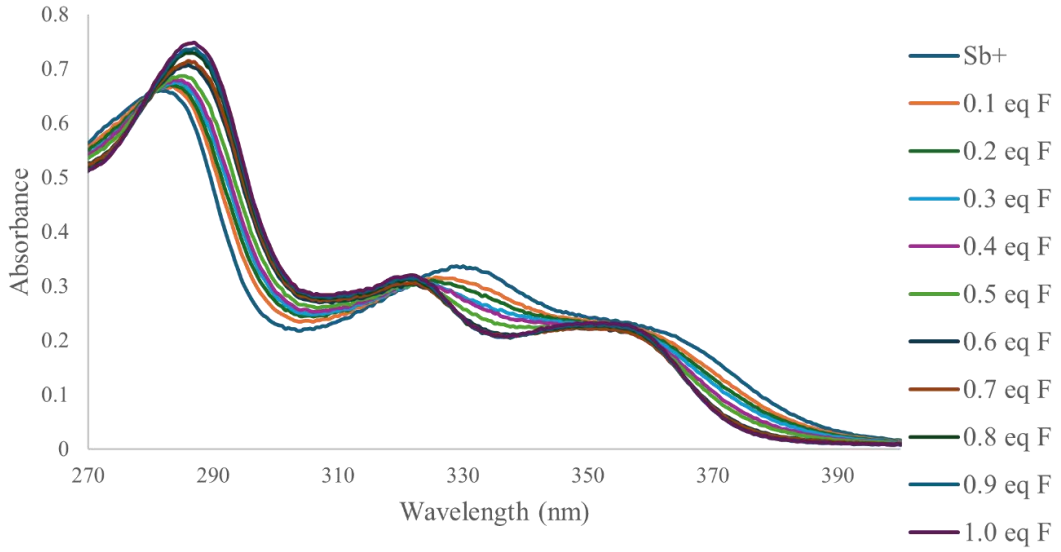

Figure 3. Changes in UV-Vis absorption spectra of **5** (Sb+; 3.2 x 10^{-5} M) upon titration with 0.01 M tetrabutylammonium fluoride (TBAF) in THF.

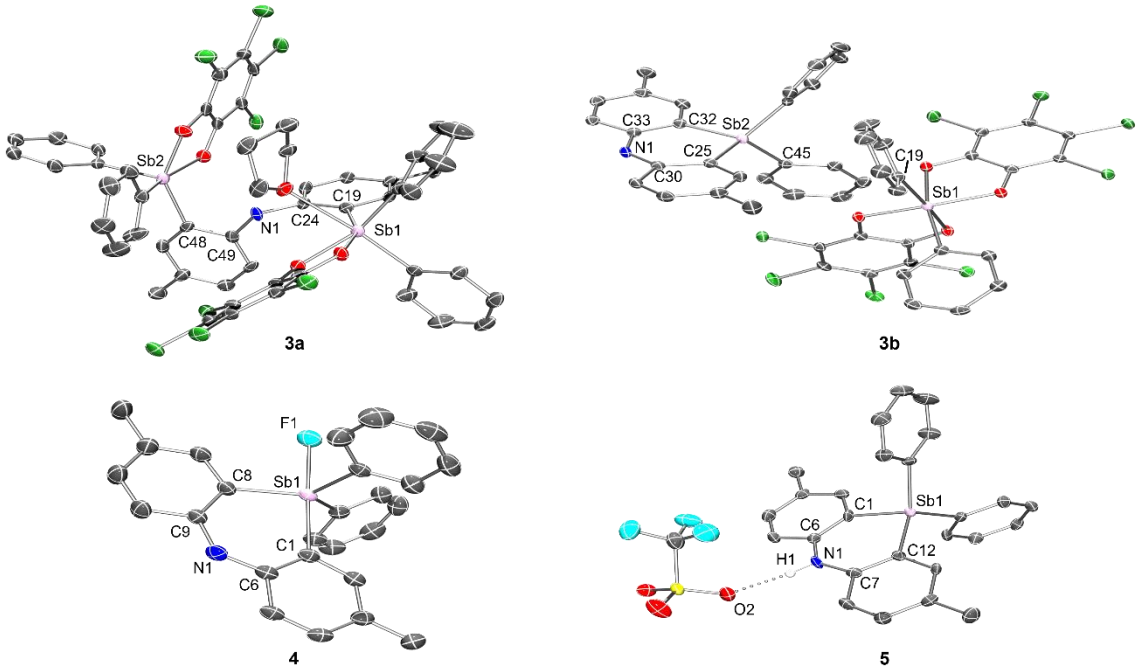

Figure 4. ORTEP drawing [23] (50% probability ellipsoids) of **3a** (top left), **3b** (top right), **4** (bottom left), and **5** (bottom right). Hydrogen atoms, the THF solvent of crystallization in **3b**, and the toluene solvent of crystallization in **4** are omitted for clarity. Selected distances in **3a** (Å): C19-Sb1, 2.161(5); C48-Sb2, 2.130(4); C24-N1, 1.438(7); C49-N1, 1.442(6). Selected distances in **3b** (Å): Sb1-C19, 2.131(3); Sb2-C45, 2.091(2); Sb2-C25, 2.063(2); Sb2-C32, 2.067(2); C30-N1, 1.386(3); C33-N1, 1.389(3). Selected distances in **4** (Å): Sb1-F1, 2.099(2); Sb1-C1, 2.160(3); Sb1-C8, 2.106(3); N1-C6, 1.390(5); N1-C9, 1.383(4). Selected distances in **5** (Å): Sb1-C1, 2.093(5); Sb1-C12, 2.094(5); N1-C6, 1.376(7); N1-C7, 1.392(7); O2-H1, 2.039(14).

*2.4. Structural Studies of Compounds **3a, 3b, 4,** and **5***

The structures of **3a**, **3b**, **4**, and **5** were determined by single-crystal X-ray diffractometry (Figure 4, Table 1). Compound **3a** features two stiborane moieties flanking a central NH unit (Figure 4, top left). One of the stiborane sites coordinates a molecule of THF (d(Sb-O) = 2.522(3) Å), and the other appears to feature a weak N→Sb interaction (2.970(4) Å). The Sb-O bond distance is consistent with other dative O→Sb(V) bonds [24]. The aryl-antimony bond distances appear to be typical and show little variation [25,26]. The structure of **3b** (Figure 4, top right) contains well-separated antimonate anion and a stibonium cation. Compared to the *bis*-stiboranyl amine isomer **3a**, the Sb-C_{Ph} bond length in the antimonate anion is typical (2.131(3)).

Table 1. Crystal data and structure refinement parameters for compounds **3-5.**

Compound	**3a**	**3b**	**4**	**5**
Chemical Formula	$C_{50}H_{33}Cl_8NO_4Sb_2$	$C_{50}H_{33}Cl_8NO_4Sb_2$	$C_{26}H_{23}FNSb$	$C_{27}H_{23}F_3NO_3SSb$
Formula Mass	1238.94	1238.94	490.24	620.3
Temperature	110.0 K	110.0 K	110.0 K	110.0 K
Wavelength	0.71073 Å	0.71073 Å	1.54178 Å	0.71073 Å
Crystal system	Triclinic	Triclinic	Monoclinic	Orthorhombic
Space group	P-1	P-1	P 1 21/n 1	Fdd2
a/Å	12.8503(18)	10.7400(7)	11.9708(10)	27.707(2)

b/Å	15.467(2)	12.2924(8)	15.2145(12)	34.928(3)
c/Å	17.832(3)	20.5918(14)	14.0910(11)	10.4825(9)
α	72.453(2)°	106.8240(10)°	90°	90°
β	77.770(2)°	98.9170(10)°	106.927(2)°	90°
γ	83.740(2)°	93.5010(10)°	90°	90°
Volume	3298.7(8) $Å^3$	2554.5(3) $Å^3$	2455.2(3) $Å^3$	10144.4(15) $Å^3$
Z	2	2	4	16
Density (calculated)	1.320 Mg/m^3	1.704 Mg/m^3	1.451 Mg/m^3	1.625 Mg/m^3
Absorption coefficient	1.182 mm^{-1}	1.526 mm^{-1}	9.098 mm^{-1}	1.222 mm^{-1}
F(000)	1300	1300	1084	4960
Crystal size	0.286 x 0.099 x 0.048 mm^3	0.324 x 0.224 x 0.042 mm^3	0.031 x 0.028 x 0.017 mm^3	0.146 x 0.094 x 0.053 mm^3
Theta range for data collection	1.837 to 24.725°	1.050 to 27.500°	4.276 to 75.810°	2.158 to 24.998°
Reflections collected	49864	30344	26273	58166
Independent reflections	11139 [R(int) = 0.0564]	11587 [R(int) = 0.0226]	5040 [R(int) = 0.0294]	4478 [R(int) = 0.0392]
Absorption correction	Semi-empirical from equivalents	Semi-empirical from equivalents	Semi-empirical from equivalents	Semi-empirical from equivalents
Max. and min. transmission	0.4897 and 0.4325	0.7458 and 0.6250	0.4716 and 0.3155	0.4240 and 0.3759
Data / restraints / parameters	11139 / 0 / 633	11587 / 0 / 633	5040 / 88 / 316	4478 / 1 / 327
Goodness-of-fit on F^2	1.036	1.03	1.143	1.341
Final R indices [I>2sigma(I)]	R_1 = 0.0411, wR_2 = 0.0926	R_1 = 0.0233, wR_2 = 0.0545	R_1 = 0.0297, wR_2 = 0.0712	R1 = 0.0241, wR2 = 0.0483
R indices (all data)	R_1 = 0.0608, wR_2 = 0.1013	R_1 = 0.0283, wR_2 = 0.0571	R_1 = 0.0334, wR_2 = 0.0753	R1 = 0.0269, wR2 = 0.0500
Absolute structure parameter	n/a	n/a	n/a	0.012(5)
Extinction coefficient	n/a	n/a	n/a	n/a
Largest diff. peak and hole	2.047 and -1.434 $e.Å^{-3}$	0.791 and -0.430 $e.Å^{-3}$	1.348 and -0.514 $e.Å^{-3}$	0.440 and -0.479 $e.Å^{-3}$
CCDC number	1901509	1901508	1901507	1901510

An XRD study of **4** (Figure 4, bottom left) confirmed the formation of the Sb-F bond (Sb1-F1, 2.099(2) **Å)**, leading to a five-coordinate Sb(V) product with a slightly distorted trigonal bipyramidal geometry (τ = 0.85) [27]. Installation of the fluoride to form the fluorostiborane **4** causes an asymmetry of the intraring Sb-C bond lengths, with the Sb-C *trans* to the fluoride having

lengthened by ca. 0.06 Å (Sb1-C1, 2.160(3) Å) *versus* the Sb-C bond which lies approximately *trans* to the empty site (Sb1-C8, 2.106(3) Å).

The structures of the cation in **4** (Figure 4, bottom right) and **5** (Figure 4, bottom) are quite similar. Notably, the central six membered ring is completely planar and the intraring C-N and Sb-C bond lengths are shortened. The C-N bond lengths in the cation of **4** and **5** are in the narrow 1.38-1.39 Å range, which is ca. 0.05-0.06 Å shorter *versus* those in the *bis*-stiboranyl amine **3a** (1.438(7) and 1.442(6) Å). The C-N distances in **4** are ca. 1.39-1.40 Å. This is also similar to the C-N distances in **E** (ca. 1.40 Å) [17].

3. Conclusion.

In summary, we discovered that although oxidation of a *bis*-2-stibinoaryl amine (**2**) with chloranil did lead to the desired molecule (**3a**) with two Sb(V) Lewis acids flanking a central NH site, spontaneous isomerization of **3a** to an ionic, tetraarylstibonium antimonate isomer (**3b**) prevents the study and use of **3a** as a potential fluoride capture agent. The isomerization proceeds with the cyclization of the diarylamine core. It is possible that the use of a different diarylamine framework that is restricted from such isomerization by the presence of additional covalent linkages, perhaps analogous to the known polycyclic diarylamido-centered PNP pincer ligands [16,28-31] could provide a promising alternative.

4. Experimental

4.1. General considerations. Unless otherwise stated, all experiments were carried out using standard glovebox and Schlenk line techniques under a dry argon atmosphere. C_6D_6 was dried over NaK, benzophenone, and 18-crown-6, distilled, and stored over molecular sieves in an argon glovebox prior to usage. All other deuterated solvents were degassed and stored over molecular sieves. Diethyl ether, tetrahydrofuran, and pentane were dried and deoxygenated using a PureSolv MD-5 solvent purification system and were stored over molecular sieves in an argon-filled

glovebox. Ph_2SbCl was prepared *via* reaction of neat $SbPh_3$ and $SbCl_3$ in a 2:1 ratio [32]. Compound **1** was prepared via an adapted literature procedure [33]. NMR spectra were recorded on a Varian iNova 500 ($^{31}P\{^1H\}$ NMR, 202.276 MHz; $^{13}C\{^1H\}$ NMR, 125.670 MHz; ^1H NMR, 499.678 MHz, ^{19}F NMR, 470.385 MHz) and Bruker 400 spectrometer (^1H NMR, 400.09 MHz; ^{13}C NMR, 100.60 MHz, ^{19}F NMR (376.498 MHz) spectrometers in given solvents. Chemical shifts are reported in ppm (δ). $^{13}C\{^1H\}$ and ^1H NMR spectra were internally referenced to residual solvent resonances [34]. In reporting spectral data, the following abbreviations were utilized: s = singlet; d = doublet; t = triplet; dd = doublet of doublets; m = multiplet. Infrared spectra were collected on an Agilent CARY FT-IR spectrometer. Elemental analyses were performed by CALI, Inc. (Highland Park, NJ, USA). Mass spectrometry was performed by the Laboratory for Biological Mass Spectrometry at Texas A&M University.

4.2. Synthesis of $SbPh_2Cl$: In a 20 mL scintillation vial, equipped with a magnetic stir bar, $SbPh_3$ (4.90 g, 13.9 mmol) and $SbCl_3$ (1.58 g, 6.93 mmol) were combined and left to stir. The solids gradually became a homogenous, golden oil that was left to stir for 16 h before being removed from the stir plate. The oil was left to stand until it had solidified, after which the solid was removed from the vial to give the product as an off-white solid. Yield: 6.47 g (100%). ^1H NMR (400 MHz, C_6D_6): δ 7.47 – 7.42 (m, 4H, Sb–Ph), 7.10 – 6.99 (m, 6H, Sb–Ph). $^{13}C\{^1H\}$ NMR (101 MHz, C_6D_6): δ 145.4 (s), 134.7 (s), 130.0 (s), 129.3 (s). **Note**: The oil must be left to solidify to yield a pure product. $^{13}C\{^1H\}$ NMR spectroscopy analysis of the oil reveals a mixture of $SbPh_xCl_{3-x}$ species (see SI for more details). $^{13}C\{^1H\}$ NMR (101 MHz, C_6D_6) for $SbPh_3$: δ 138.9 (s), 136.6 (s), 129.2 (s), 128.9 (s). $^{13}C\{^1H\}$ NMR (101 MHz, C_6D_6) for $SbCl_2Ph$: δ 153.3 (s), 132.8 (s), 131.2 (s), 129.4 (s).

4.3. Synthesis of **2**: To a 200 mL Schlenk flask equipped with a magnetic stir bar was added **1** (2.18 g, 6.13 mmol) and 50 mL diethyl ether. To this stirring solution was slowly added a 2.5 M solution of *n*-butyllithium in hexanes (7.44 mL, 18.6 mmol) causing the solution to become slightly yellow. The solution was allowed to stir for 3 h, and then Ph_2SbCl (3.83 g, 12.3 mmol) was added

as a suspension in 3 mL of THF, causing the solution to become a cloudy, bright yellow. After the addition was completed, the suspension was allowed to stir for 16 h. To the suspension was then added 1 mL of degassed H_2O, causing the mixture to become a light yellow, homogeneous solution, which was then allowed to stir for 1 h. Solvent was then removed under reduced pressure to yield a waxy yellow residue which was dissolved in a minimal amount of fluorobenzene and filtered through a frit containing Celite and silica. The fluorobenzene was removed *in vacuo* to give a waxy yellow solid which was washed with 20 mL of *iso*octane and dried. The resultant solid was dissolved in a minimal of diethyl ether, layered with *iso*octane, and recrystallized at -37 ºC over 12 h. The solvent was decanted, and the solids were washed with *iso*octane then pentane and dried, providing the product as a white, free-flowing solid. Yield: 1.407 g (31%).^{1}H NMR (400 MHz, $CDCl_3$): δ 7.39 – 7.35 (m, 8H, Sb-Ph), 7.31 – 7.25 (m, 12H, Sb-Ph), 6.97 – 6.91 (m, 4H, Ar CH), 6.72 (d, 2 H, J_{HH} = 8 Hz, 2H, Ar CH), 5.38 (s, 1H, N-H) 2.13 (s, 6H, benzylic CH_3). $^{13}C\{^1H\}$ NMR (101 MHz, $CDCl_3$): δ 147.1, 138.0, 137.5, 136.5, 132.6, 132.0, 130.9, 129.0, 128.6, 120.5, 20.9 (benzylic CH_3). ATR-IR (cm^{-1}): $\nu_{N\text{-}H}$- 3338 cm^{-1} HRMS (ESI^+) m/z $[M+H]^+$: calc'd for $C_{38}H_{33}NSb_2$: 748.0766, found 748.0719.

4.4. Synthesis of **3a**: To a 20 mL scintillation vial equipped with a magnetic stir bar was added **2** (65 mg, 0.0857 mmol) and *o*-chloranil (42 mg, 0.171 mmol), followed by 4 mL of toluene to give a red solution that gradually turned a pale yellow over the course of 15 minutes. The solvent was removed under reduced pressure, and the remaining solid was rinsed with pentane (1 × 2 mL) before drying further to reveal the product as a pale-yellow solid (88 mg, 83%). White, single crystals suitable for X-ray diffraction were grown from a THF/pentane mixture at -38 ºC. ^{1}H NMR (C_6D_6, 400 MHz): δ 9.03 (s, 1H, N–H), 7.72 (br s, 8H), 7.22 (d, J_{HH} = 8 Hz, 2H, Ar CH), 7.07 – 6.88 (m, 16 H), 1.78 (s, 6H, benzylic CH_3). $^{13}C\{^1H\}$ NMR (C_6D_6, 101 MHz): δ 147.3, 144.7, 135.0, 134.5, 134.3, 133.9, 133.7, 132.0, 129.9, 129.3, 125.7, 124.7, 121.4, 117.1, 20.5. ATR-IR (cm^{-1}): $\nu_{N\text{-}H}$- 3193 cm^{-1}.

4.5. Synthesis of **3b**: To a 20 mL scintillation vial equipped with a magnetic stir bar was added **2** (64 mg, 0.0857 mmol) and *o*-chloranil (42 mg, 0.171 mmol), followed by 6 mL of THF to give an orange solution. The solution was left to stir overnight (*ca*. 16 h), during which the color changed to very pale yellow. The solvent was removed under reduced pressure, and the residue was washed with Et_2O (2 × 2 mL) before drying further to reveal the product as a pale yellow solid (97 mg, 92%).^{1}H NMR (400 MHz, DMSO-d_6): δ 9.79 (s, 1H, N-H), 7.81 (m, 4H), 7.65 (br, 8H), 7.55 (m, 4H), 7.43 (m, 6H), 7.36 (d, J = 8 Hz, 2H, Ar CH), 7.29 (d, J = 8 Hz, 2H, Ar CH), 2.24 (s, 6H, benzylic CH_3). ^{13}C{^{1}H} NMR (101 MHz, DMSO-d_6): δ 147.5, 146.0, 144.7, 144.2, 134.8, 134.8, 134.3, 132.5, 132.2, 130.4, 130.3, 130.1, 129.0, 119.0, 118.2, 117.2, 116.0, 115.2, 105.3, 20.1. ATR-IR (cm^{-1}): $\nu_{N\text{-}H}$- 3334 cm^{-1}. Elem Anal Found (calc): C: 49.46 (49.47) H: 3.12 (3.15).

4.6. Variable temperature NMR study of **3b**: To a J. Young tube was added **3b** (17.0 mg, 0.013 mmol) and THF-d_8 resulting in a clear, colorless solution. ^{1}H NMR spectra taken at variable temperatures (25, 0, -20, and -40 °C) revealed no changes in solution symmetry on the NMR timescale.

4.7. General procedure for solvent dependent isomerization experiments: To a J. Young tube was added 11 mg of **3a**, followed by 1.5 μL of mesitylene as an internal standard. Afterwards, 500 μL of the appropriate solvent was added to each tube. The tube was shaken to ensure complete solvation of the material, and then analyzed by ^{1}H NMR spectroscopy (*ca.* 10 min after mixing). The tubes were continued to be monitored by ^{1}H NMR spectroscopy at various timepoints. All concentrations (including initial [**3a**]$_0$) of isomers were determined by integrating the aryl–CH_3 resonances against the mesitylene CH_3 resonance. For samples where the ionic isomer had limited solubility, DMSO-d_6 was added after the final timepoint to confirm its presence and ratio to the neutral isomer.

4.8. Synthesis of **4**: To a 20 mL scintillation vial equipped with a magnetic stir bar was added **3b** (122 mg, 0.098 mmol) and 4 mL THF. To this stirring suspension was then added CsF (15 mg,

0.099 mmol), causing the suspension to form a homogeneous solution. The resultant solution was then stirred for 16 h, and then volatiles were removed under reduced pressure, forming an off-white residue. The residue was then extracted with 5 mL PhF and filtered through a plug of Celite to give a clear, colorless solution. Volatiles were removed *in vacuo* to provide the product as a free-flowing, white powder (46 mg, 87%). ^{1}H NMR (400 MHz, $CDCl_3$): δ 7.92 – 7.85 (m, 4H, $SbPh_2$), 7.45 – 7.37 (m, 6H, $SbPh_2$), 7.12 (dd, J_1 = 8 Hz, J_2 = 2 Hz, 2H), 6.82 (d, J_1 = 8 Hz, 2H), 6.68 (br s, 1H, N–H), 2.20 (s, 6H, Ar-CH_3). ^{19}F{^{1}H} NMR (376 MHz, $CDCl_3$): δ -100.4. ^{1}H NMR (400 MHz, THF-d_8) δ 8.31 (s, 1H, N–H), 7.93 – 7.84 (m, 4H, $SbPh_2$), 7.58 – 7.46 (m, 2H, Ar CH), 7.41 – 7.30 (m, 6H, Sb–Ph), 7.08 (dd, J_1 = 8 Hz, J_2 = 2 Hz, 2H, Ar CH), 6.92 (d, J = 8 Hz, 2H, Ar CH), 2.14 (s, 6H, benzylic CH_3). ^{13}C{^{1}H} NMR (101 MHz, THF-d_8) δ 148.1 (s), 138.4 (s), 138.1 (s), 137.3 (s), 132.6 (s), 130.7 (s), 129.0 (s), 128.8 (s), 117.9 (br s), 117.3 (s), 20.44 (s). ^{19}F{^{1}H} NMR (376 MHz, THF-d_8): δ -105.1HRMS (ESI^+) m/z $[M+H]^+$: calc'd for $C_{26}H_{23}FNSb$: 491.0851, found 491.0847.

4.9. Synthesis of **5**: To a J. Young tube was added **4** (22 mg, 0.045 mmol) and $CDCl_3$, forming a clear, colorless solution. To this solution was added Me_3SiOTf (12 µL, 0.066 mmol) resulting in a slight color change to yellow. ^{1}H and ^{19}F NMR spectroscopy evidenced a full, clean conversion to the product, along with formation of one equivalent of Me_3SiF. The contents of the tube were then filtered through a pad of celite into a 20 mL scintillation vial, and the solvent was removed under reduced pressure. The residue was washed with pentane (3 × 1 mL) and dried further to reveal the product as an off-white solid (24 mg, 86%). Colorless crystals suitable for X-ray diffraction were grown from a toluene/pentane vapor diffusion at room temperature. ^{1}H NMR (400 MHz, $CDCl_3$) δ 9.55 (s, 1H, N–H), 7.75 – 7.60 (m, 12H), 7.31 (dd, J_1 = 9 Hz, J_2 = 2 Hz, 2H, Ar CH), 7.27 (br s, 2H, Ar CH), 2.28 (s, 6H). ^{13}C{^{1}H} NMR (101 MHz, $CDCl_3$) δ 144.2 (s), 136.4 (s), 135.1 (s), 134.0 (s), 133.4 (s), 132.2 (s), 131.4 (s), 123.0 (s), 120.7 (s), 97.4 (s), 20.6 (s). ^{19}F{^{1}H}

NMR (376 MHz, $CDCl_3$): δ -76.9. HRMS (ESI^+) m/z $[M]^+$: calc'd for $C_{26}H_{23}NSb$: 470.0863, found 470.0855.

Appendix A. Supplementary data.

Supplementary data to this article containing graphical spectral data, and the details of X-ray structure determinations can be found online. CCDC 1901507-1901510 contain the supplementary crystallographic data for compounds **4**, **3b**, **3a**, and **5**, respectively. These data can be obtained free of charge via http://www.ccdc.cam.ac.uk/conts/retrieving.html, or from the Cambridge Crystallographic Data Centre, 12 Union Road, Cambridge CB2 1EZ, UK; fax: (+44) 1223-336-033; or e-mail: deposit@ccdc.cam.ac.uk.

Acknowledgment. We are grateful for the support of this work by the US National Science Foundation (grants CHE-1300299 and CHE-2102324 to O.V.O., and an NSF LSAMP Fellowship to A.J.K. via grant HRD-1406755). We would like to thank Prof. François Gabbaï for helpful discussions and for assistance with some drawings, and Dr. Gyeongjin Park for her assistance with designing and interpreting fluoride capture experiments.

References

[1] W. Levason, G. Reid, Coord. Chem. Rev. 250 (2006) 2565-2594.

[2] S.L. Benjamin, G. Reid, Coord. Chem. Rev. 297-298 (2015) 168-180.

[3] J.S. Jones, F.P. Gabbaï, Acc. Chem. Res. 49 (2016) 857–867.

[4] S. Furan, E. Hupf, J. Boidol, J. Brünig, E. Lork, S. Mebs, J. Beckmann, Dalton Trans. 48 (2019) 4504-4513.

[5] S.L. Benjamin, T. Krämer, W. Levason, M.E. Light, S.A. Macgregor, G. Reid, J. Am. Chem. Soc. 138 (2016) 6964–6967.

[6] Y.H. Lo, F.P. Gabbaï, Organometallics 37 (2018) 2500-2506.

[7] C.-H. Chen, F.P. Gabbaï, Angew. Chem. Int. Ed. 56 (2017) 1799-1804.

[8] B.L. Murphy, F.P. Gabbaï, J. Am. Chem. Soc. 145 (2023) 19458–19477.

[9] C.R. Wade, I.-S. Ke, F.P. Gabbaï, Angew. Chem. Int. Ed. 51 (2012) 478 –481.

[10] A.M. Christianson, F.P. Gabbaï, Chem. Commun. 53 (2017) 2471-2474.

[11] J.L. Beckmann, J. Krieft, Y.V. Vishnevskiy, B. Neumann, H.-G. Stammler, N.W. Mitzel, Angew. Chem. Int. Ed. 62 (2023) e202310439.

[12] J. Qiu, B. Song, X. Li, A. F. Cozzolino, Phys. Chem. Chem. Phys. 20 (2018) 46-50.

[13] M. Hirai, F.P. Gabbaï, Angew. Chem. Int. Ed. 54 (2015) 1205-1209.

[14] C.-H. Chen, F.P. Gabbaï, Angew. Chem. Int. Ed. 56 (2017) 1799-1804.

[15] J.J. Davidson, J.C. DeMott, C. Douvris, C.M. Fafard, N. Bhuvanesh, C.-H. Chen, D.E. Herbert, C.-I Lee, B.J. McCulloch, B.M. Foxman, O.V. Ozerov, Inorg. Chem. 54 (2015) 2916-2935.

[16] B. Zhou, F.P. Gabbaï, J. Am. Chem. Soc. 145 (2023) 13758-13767.

[17] A.J. Kosanovich, A.M. Jordan, N. Bhuvanesh, O.V. Ozerov, Dalton Trans. 47 (2018) 11619-11624.

[18] V.K. Cherkasov, G.A. Abakumov, E.V. Grunova, A.I. Poddel'sky, G.K. Fukin, E.V. Baranov, Y.V. Kurskii, L.G. Abakumova, Chem. Eur. J. 12 (2006) 3916-3927.

[19] A.I. Poddel'sky, I.V. Smolyaninov, N.V. Somov, N.T. Berberova, V.K. Cherkasov, G.A. Abakumov, J. Organomet. Chem. 695 (2010) 530-536.

[20] A.M. Christianson, E. Rivard, F.P. Gabbaï, Organometallics 36 (2017) 2670-2676.

[21] M. Hirai, M. Myahkostupov, F.N. Castellano, F.P. Gabbai, Organometallics 35 (2016) 1854-1860.

[22] I.-S. Ke, M. Myahkstupov, F.N. Castellano, F.P. Gabbai, J. Am. Chem. Soc. 134 (2012) 15309-15311.

[23] L. Farrugia, J. Appl. Crystallogr. 30 (1997) 565-566.

[24] J.E. Smith, F.P. Gabbaï, Organometallics 42 (2023) 240–245.

[25] M. Hirai, F.P. Gabbaï, *Angew. Chem. Int. Ed.* 54 (2015) 1205–1209.

[26] C.-H. Chen, F.P. Gabbaï, *Angew. Chem. Int. Ed.* 56 (2017) 1799–1804.

[27] A.W. Addison, T.N. Rao, J. Reedijk, J. van Rijn, G.C. Verschoor, *J. Chem. Soc., Dalton Trans.* 13 (1984) 1349–1356.

[28] W. Weng, C. Guo, C.P. Moura, L. Yang, B.M. Foxman, O.V. Ozerov, Organometallics 24 (2005) 3487-3499.

[29] J. Zhai, F. You, S. Xu, A. Zhu, X. Kang, Y.-M. So, X. Shi. Inorg. Chem. 61 (2022) 1287-1296.

[30] D. Sahoo, C. Yoo, Y. Lee. J. Am. Chem. Soc. 140 (2018) 2179-2185.

[31] G. Kleinhans, A.J. Karhu, H. Boddaert, S. Tanweer, D. Wunderlin, D.I. Bezuidenhout. Chem. Rev. 123 (2023) 8781-8858.

[32] M. Nunn, D.B. Sowerby and D.M. Wesolck. J. Organomet. Chem. 251 (1983) C45-C46.

[33] H. Gilman and E.A. Zuech, J. Org. Chem. 26 (1961) 3481-3484.

[34] G.R. Fulmer, A.J.M. Miller, N.H. Sherden, H.E. Gottlieb, A. Nudelman, B.M. Stoltz, J.E. Bercaw, K.I. Goldberg, Organometallics 29 (2010) 2176-2179.